Optics Communications 479 (2021) 126377

Contents lists available at ScienceDirect

Optics Communications

journal homepage: www.elsevier.com/locate/optcom

# Gain-coupled 770 nm DFB semiconductor laser based on surface grating

Chunkao Ruan [a,b], Yongyi Chen [a,c,*], Feng Gao [a], Li Qin [a,c], Dezheng Ma [a,b], Peng Jia [a], Chao Chen [a], Hao Wu [a], Xia Liu [a,b], Yugang Zeng [a], Xing Zhang [a], Yue Song [a], Yongqiang Ning [a], Lijun Wang [a,c]

[a] State Key Laboratory of Luminescence and Application, Changchun Institute of Optics, Fine Mechanics and Physics, Chinese Academy of Sciences, Changchun 130033, China

[b] University of Chinese Academy of Sciences, Beijing 100049, China

[c] Peng Cheng Laboratory No.2, Xingke 1st Street, Nanshan, Shenzhen, China

ARTICLE INFO

*Keywords:*
Surface grating
Gain-coupled
770 nm
Distributed-feedback

ABSTRACT

Single-longitudinal-mode gain-coupled distributed feedback (DFB) lasers based on high-order gain-coupled surface gratings emitting at 770 nm window are implemented. The periodic surface metal p-contact with insulated grating grooves realizes a gain coupled mechanism. Our devices provided a single longitudinal mode with the maximum CW output power up to 116.8 mW@400 mA with facet coated (HR>99%, AR<0.5%), 3 dB linewidth is 0.26 pm and SMSR is 36 dB. Due to easy-to-manufacture technology and stable performance, it provides a practical gain-coupled distributed feedback laser emitting at 770 nm region manufacturing method for commercial applications.

## 1. Introduction

Distributed Feedback (DFB) semiconductor laser is compact and provides a high degree of spectral selection [1], could be applied in many fields, such as spectroscopy [2], pumping sources [3], material processing [4], integrated optics [5], and lidar [2,6,7]. The laser emitting at 770 nm which corresponds to the transition lines of Mg, K, Fe, Ni and other atoms, has many applications [8], such as, helioseismology studies using resonance cells [9], the estimation of solar atmospheric parameters [10], and pumps for alkali metal atomic clocks [11]. However, even though the wavelength around 780 nm [12,13] and 785 nm [14,15] DFB lasers are reported, 770 nm DFB lasers remain unexplored except for the DBR arrays [16] and the VECSEL arrays [17].

DFB lasers can be divided into refractive index-coupled and gain-coupled DFB lasers according to the coupling type. A problem inherent in index-coupled DFB lasers with uniform refractive index is the generation of two degenerate modes [1]. The introduction of phase shift grating could effectively eliminate mode degradation [18], but may suffer from space hole burning (SHB) at high output power [19,20].

In previous studies, we reported gain-coupled DFB (GC-DFB) laser based on periodic gain (or loss) is another solution to obtain single longitudinal mode [21,22]. The implementation of the gain-coupled mechanism could eliminate mode degradation [23], achieve high single-mode yield [24], be facet immunity [25], and be insensitivity to external feedback [26]. Compared with the index-coupled DFB which require secondary epitaxial growth technology and holographic lithography technology [13], this method offers a new way to fabricate single longitudinal mode DFB lasers that are at the same power level as commercial products [27,28].

In this paper, a regrowth-free GC-DFB laser based on gain-coupled high order surface gratings emitting at 770 nm region was demonstrated. The combined effect of the periodic surface high-order gain-coupled gratings and the insulated grating grooves fabricated only by i-line lithography would cause a periodic injection of current, resulting in gain contrast in the quantum wells, forming a gain coupled mechanism [21]. Stable, single-longitudinal-mode and high SMSR (36 dB), and 3 dB linewidth (0.26 pm) were achieved. The SMSR was better than that of other high-order surface gain-coupled gratings [22,29]. The GC-DFB laser was emitting at 770 nm, which is attractive for atomic clocks for potassium D1 lines [11]. Due to easy-to-manufacture technology and stable performance, it provides a practical gain-coupled distributed feedback laser manufacturing method for commercial applications.

## 2. Structure and fabrication

The chip structure of the laser is shown in Table 1. The devices used AlGaAs double quantum wells (QWs) emitting at 770 nm as the gain material.

A schematic diagram of the DFB laser is shown in Fig. 1(a). The active region of the DFB laser are double quantum wells of AlGaAs.

* Corresponding author at: State Key Laboratory of Luminescence and Application, Changchun Institute of Optics, Fine Mechanics and Physics, Chinese Academy of Sciences, Changchun 130033, China.
*E-mail addresses:* chenyy@ciomp.ac.cn (Y. Chen), gaofeng15@mails.ucas.ac.cn (F. Gao), zengyg@ciomp.ac.cn (Y. Zeng).

https://doi.org/10.1016/j.optcom.2020.126377
Received 13 July 2020; Received in revised form 12 August 2020; Accepted 13 August 2020
Available online 14 August 2020

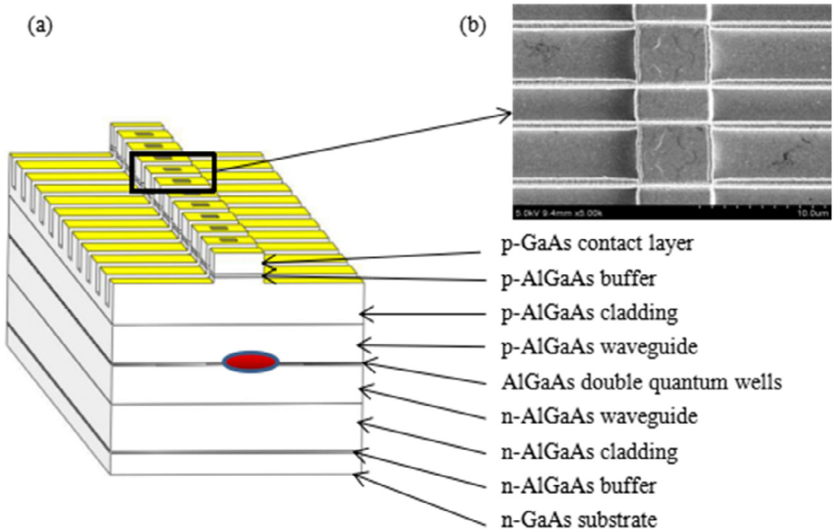


**Fig. 1.** (a) Device schematic; (b) Scanning electron microscope image of device.

**Table 1**
Epitaxial structures for the 770 nm chip.

| Material | Structure | Thickness (um) | Type |
|---|---|---|---|
| GaAs | Contact layer | 0.2 | P |
| Al(x)GaAs | Buffer | 0.05 | P |
| Al(x)GaAs | Cladding | 1.1 | P |
| Al(x)GaAs | Waveguide | 0.9 | P |
| Al(x)GaAs | Double quantum wells | 0.0055*2 | Undoped |
| Al(x)GaAs | Waveguide | 0.9 | N |
| Al(x)GaAs | Cladding | 1.1 | N |
| Al(x)GaAs | Buffer | 0.05 | N |
| GaAs | Substrate | | N |

The ridge width is 6 μm. The surface gratings period is 9.02 μm. The width of the gratings grooves filled with silica is 3 μm. The grating etched depth is designed to be 800 nm (fabricated as 786 nm), and the total etched depth is designed to be 1500 nm (fabricated as 1487 nm). Fig. 1(b) is the scanning electron microscope image of the device. As shown in Fig. 1, periodic p-contacts and periodic gratings insulated by silica caused periodic injection current. The periodic injection of current into the surface grating causes the nonuniform distribution of carriers and current densities in the quantum wells, thereby forming a gain contrast and a gain coupled mechanism in the quantum wells, as shown in Fig. 2. Considering the gain-coupled effect and index-coupled effect both introduced by surface gratings' grooves, we should carefully design to avoid too much index coupling effect to prevent high order scattering, which may cause additional optical losses and increase the threshold.

$\kappa$ represents the coupling coefficient [21]:

$$\kappa = k_0 \Gamma \left(\Delta n \frac{\sin(\frac{l\pi}{\Lambda} L_g)}{l\pi} + i\frac{\Delta g}{4k_0}\right) \quad (1)$$

Where, $k_0 = 2\pi/\lambda_0$ is the vacuum wave number for the vacuum wavelength $\lambda_0$. $\Gamma$ is the optical confinement factor of the etched grooves in our device. $\Delta n$ is the refractive index change in the waveguide. $L_g$ represents the grating's groove width. And $\Lambda$ is the period for the $l$ order grating ($\Lambda = l\lambda/2n_{\mathrm{eff}}$). $\Delta g$ represents the gain/loss change in the waveguide.

To calculate coupling coefficient $\kappa$, we need to know the values of $\Gamma$, $\Delta n$, and $\Delta g$, as shown in Eq. (1), where $\Gamma = 0.002$ is the optical confinement factor of the etched grooves in our device, and $\Delta n = 0.0004$ are calculated by the commercial software COMSOL Multiphysics. As $\Delta g = 199/cm$, calculated by PICS3D as shown in Fig. 2(c), is the gain change in the waveguide. Substituting the above values into Eq. (1), we can get $\kappa = 4.80\times10^{-5} + 9.95\times10^{-2} i$ (cm$^{-1}$). The real and imaginary parts of $\kappa$ are not 0, but the ratio of real and imaginary parts of $\kappa$ is only $4.82\times10^{-4}$. Considering that the injected current would change the refractive index, a simulation was carried out by using PICS3D, as shown in Fig. 2(d). The maximum refractive index variation within the quantum well is only 0.0000884, the $\kappa L$ brought by the index variation is only $1.06*10^{-5}$, which is much weaker than the refractive index coupling effect caused by the surface grating. Meanwhile, the total $\kappa L$ is $5.86*10^{-5}$ considering all together with the surface etching induced index coupling effect. Compared with the generally single-longitudinal-mode index-coupled DFB semiconductor laser, it is usually greater than 1 [18], and even the multi-longitudinal mode index-coupled DFB laser has reached 0.3 [30]. These mean that the strength of the refractive index-coupled is negligible, and the laser is a gain-coupled DFB laser.

## 3. Result and discussion

The power–current–voltage characteristics at continuous-wave (CW) operation at 20 °C are shown in Fig. 3(a). The DFB laser cavity length is 1 mm with facet coating (HR>99%, AR<0.5%). The maximum CW power of coated DFB lasers at single longitudinal mode operation was up to 116.8 mW at 400 mA, which is better than the laterally-coupled ridge-waveguide (LC-RWG) surface gratings of the DFB lasers reported by [31]. The slope efficiency in the coated DFB lasers was 0.292 W/A. As shown in Fig. 3(b), the SMSR of coated DFB lasers at single longitudinal mode operation was up to 36 dB measured with a 5 μm core diameter fiber-linking YOKOGAWA AQ6370C optical spectrum analyzer, which is better than that of other high-order surface gain-coupled gratings [22,29].

As shown in Fig. 4, The single longitudinal mode lasing spectrum of the laser in the injection current range of 200–400 mA is excellent, and the side mode suppression ratios are all greater than 30 dB. And the tuning range of wavelength vs current is from 770.27 nm to 772.27 nm, and the total tuning range is 2 nm. As shows in Fig. 4 and Fig. 3(b), there are many small peaks which can be observed with a typical spacing of 0.069 nm, in addition to a main peak in the spectrum. This value closely matches the expected mode spacing and the resonator length of the device.

It can be seen in Fig. 4 that the lasing wavelength increases as the current increases. During testing, only the bottom of the device contacted the cooling source. The heat accumulation as the current increasing tended to red shift the quantum well's gain spectrum and also caused an increase to the refractive index, both of these reasons lead to the red shift of the lasing wavelength. In addition to the

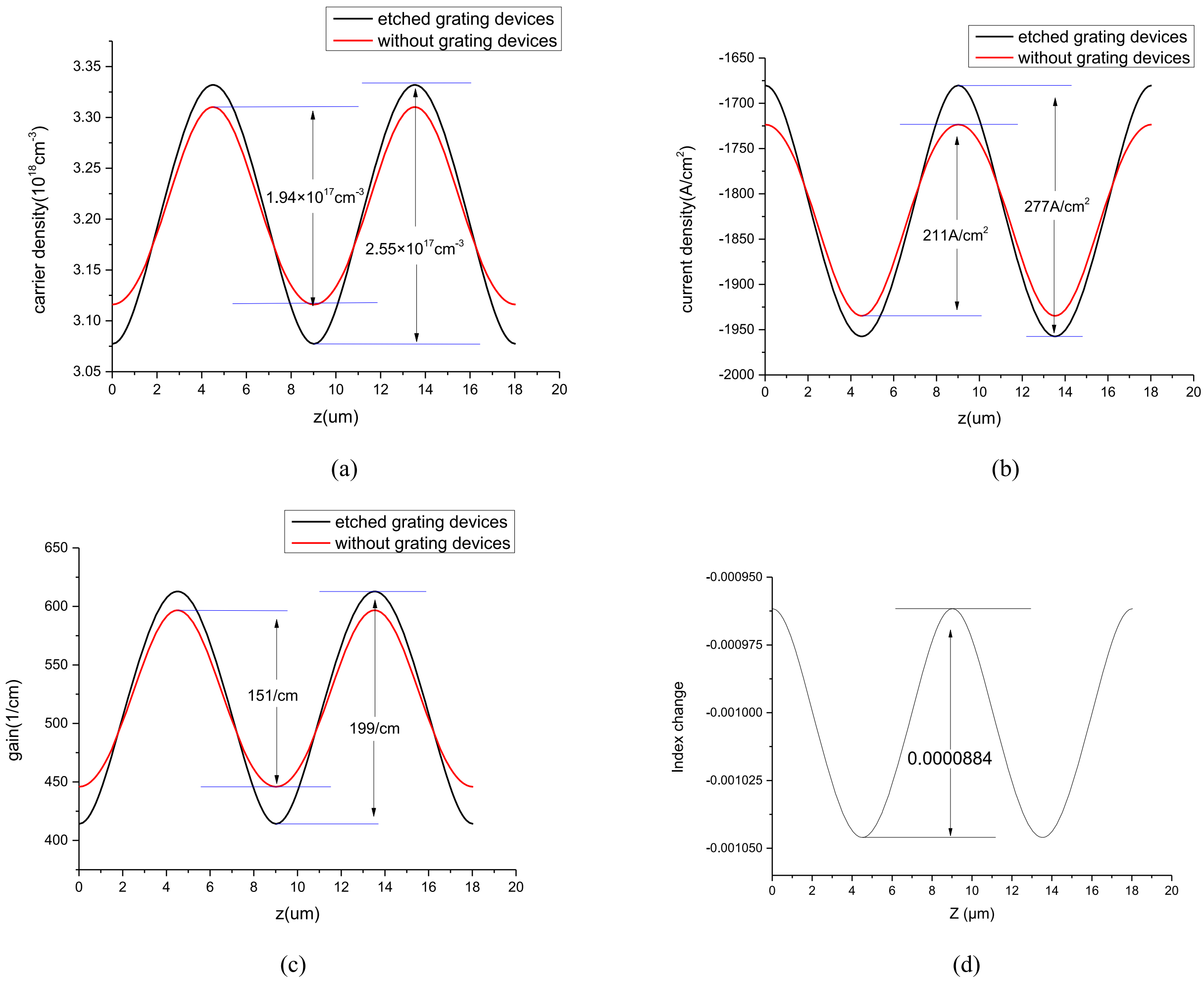


**Fig. 2.** (a) One-dimensional carrier density distribution in the quantum well for the etched grating devices and pure periodic anode devices without etched grating structures. (b) One-dimensional current density distribution in the quantum well for the etched grating devices and pure periodic anode devices without etched grating structures. (c) One-dimensional gain distribution in the quantum well for the etched grating devices and pure periodic anode devices without etched grating structures. (d) One-dimensional index change in the quantum well for the etched grating devices.

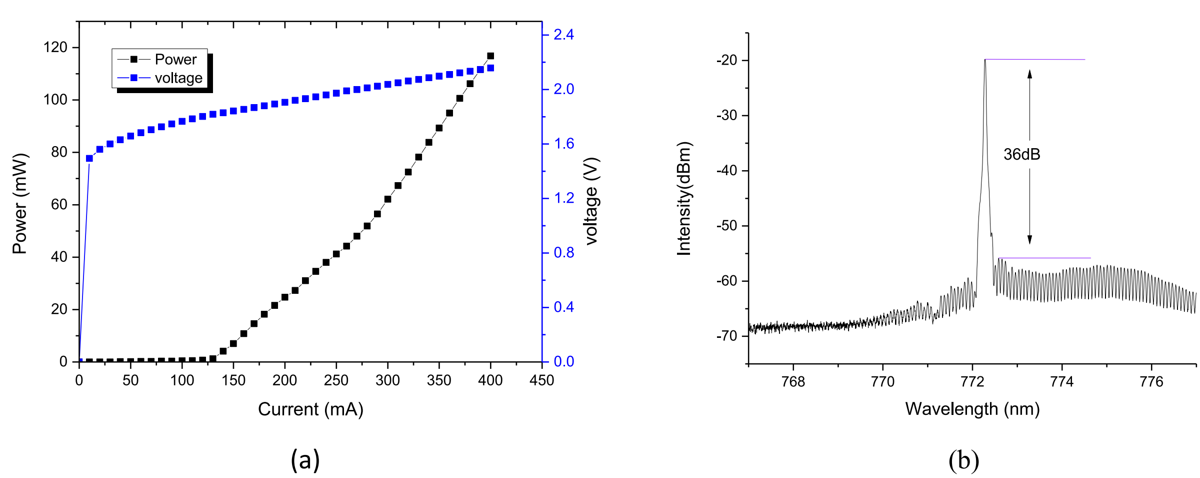


**Fig. 3.** (a) Power–voltage–current characteristics, (b) The spectrum characteristics in CW mode from DFB lasers with 1 mm cavity length.

gain-coupled effect, the device also has a mode selection mechanism from the FP cavity. This mechanism has the effect of narrowing the linewidth, meanwhile causing the tuning wavelength discontinuities, as shown in the third and fourth spectral lines in Fig. 4. Since our gain-coupled effect is relatively weak, it actually only serves as a supporting role in mode selection from the FP modes.

Fig. 5 shows the linewidth pattern of the coated DFB laser device measured by coupling the collimating laser into a Fabry–Perot (FP) interferometer (Thorlabs, 260SA200-8B). The Fabry–Perot (FP) interferometer's free spectral range is 10 GHz. So we can get from the figure that the 3 dB spectral linewidth of narrowband emission is only 0.26 pm (128 MHz) at full width at half-maximum (FWHM), which is better

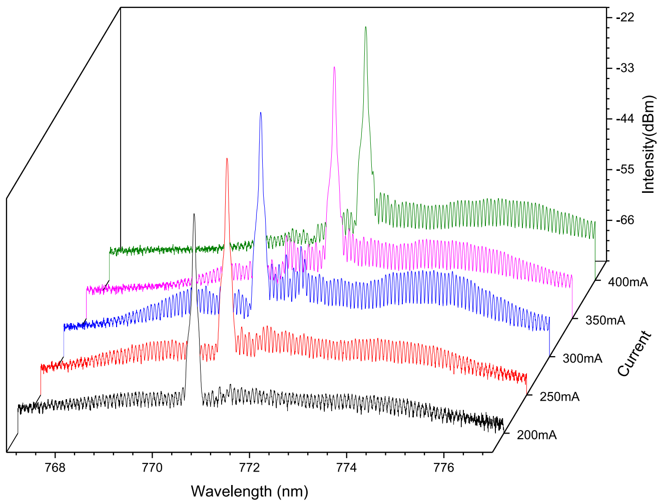


**Fig. 4.** Schematic diagram of spectrum changes with current.

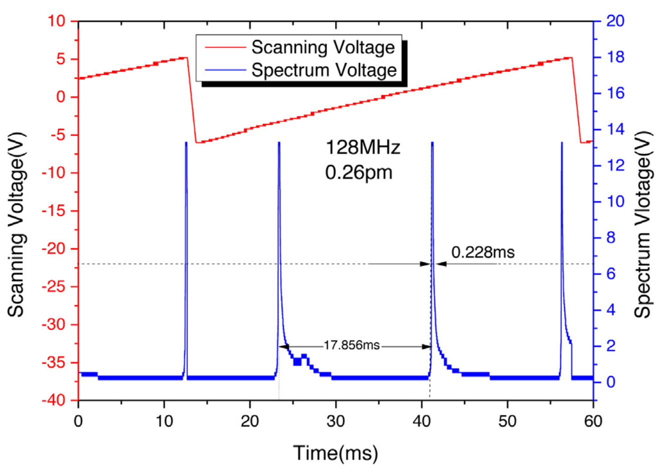


**Fig. 5.** Linewidth pattern of the coated DFB laser device.

than the previous paper 3.2 pm [21]. However, since the resolution of the instrument is 67 MHz, and 128 MHz is too close to this value, the actual linewidth may be even smaller.

## 4. Conclusion

A single-longitudinal-mode gain-coupled without-regrowth DFB semiconductor laser by only low-cost i-line lithography based on surface grating with a center wavelength of approximately 770 nm was demonstrated. Due to easy fabrication technique and stable performance, it provides a method of fabricating practical gain-coupled distributed feedback lasers emitting at 770 nm window for commercial applications. Our coated devices with 1 mm cavity length could provide stable single longitudinal mode operation with the maximum CW output power up to 116.8 mW at 400 mA, which is better than the laterally-coupled ridge-waveguide (LC-RWG) surface gratings of the DFB lasers reported in the letter by [30]. The SMSR of coated DFB lasers at single longitudinal mode operation was up to 36 dB emitting at 770 nm region. The 3 dB spectral linewidth of narrowband emission is only 0.26 pm at full width at half-maximum (FWHM).

## Declaration of competing interest

The authors declare that they have no known competing financial interests or personal relationships that could have appeared to influence the work reported in this paper.


## Funding

This work is supported by National Science and Technology Major Project of China (2016YFE0200700, 2017YFB0503100, 2017YFB0405100, 2018YFB0504600, 2018YFB2200300); Frontier Science Key Program of the President of the Chinese Academy of Sciences (QYZDY-SSW-JSC006); National Natural Science Foundation of China (NSFC) (11874353, 61935009, 61934003, 61674148, 61904179, 61727822, 61805236); Science and Technology Development Project of Jilin Province (20200401069GX, 20200401062GX); Opened Fund of the State Key Laboratory of Integrated Optoelectronics (IOSKL2018KF21); Youth Program of National Natural Science Foundation of China (61904179); Dawn Talent Training Program of CIOMP.


## References


[1] H. Kogelnik, C.V. Shank, Coupled-wave theory of distributed feedback lasers, J. Appl. Phys. 43 (5) (1972) 2327–2335.

[2] R. Nehrir, K.S. Repasky, J.L. Carlsten, Eye-safe diode-laser-based micropulse differential absorption lidar (DIAL) for water vapor profiling in the lower troposphere, J. Atmos. Ocean. Technol. 28 (2) (2011) 131–147.

[3] H. Jeon, J.M. Verdiell, M. Ziari, A. Mathur, High-power low-divergence semiconductor lasers for GaAs-based 980-nm and InP-based 1550-nm applications, IEEE J. Sel. Top. Quantum Electron. 3 (6) (1998) 1344–1350.

[4] W. Schulz, R. Poprawe, Manufacturing with novel high-power diode lasers, IEEE J. Sel. Top. Quantum Electron. 6 (2000) 696–705.

[5] Z. Zhou, B. Yin, J. Michel, On-chip light sources for silicon photonics, Light Sci. Appl. 4 (2015) e358.

[6] W. Tilma, M. Mangold, C.A. Zaugg, S.M. Link, D. Waldburger, A.398. Klenner, A.S. Mayer, E. Gini, M. Golling, U. Keller, Recent 399 advances in ultrafast semiconductor disk lasers, Light: Sci. Appl. 4004 (2015) e310.

[7] E.C. Burrows, K.Y. Liou, High resolution laser LIDAR utilising 402 two-section distributed feedback semiconductor laser as a coherent 403 source, Electron. Lett. 26 (1990) 577–579.

[8] C. Quintero Noda, H. Uitenbroek, Y. Katsukawa, et al., Solar polarimetry through the KI lines at 770 nm, Mon. Not. R. Astron. Soc. 470 (2) (2018) 1453–1461.

[9] J.R. Brookes, G.R. Isaak, d.R.H.B. Van, A resonant-scattering solar spectrometer, Mon. Not. R. Astron. Soc. 185 (1) (1978) 1–18.

[10] J.H.M.J. Bruls, R.J. Rutten, The formation of helioseismology lines. II - Modeling of alkali resonance lines with granulation, Astron. Astrophys. 265 (1992) 257–267.

[11] O. Brox, F. Bugge, A. Mogilatenko, et al., Distributed feedback lasers in the 760 to 810 nm range and epitaxial grating design, Semicond. Sci. Technol. 29 (9) (2014) 095018.

[12] T.P. Nguyen, H. Wenzel, O. Brox, et al., Spectral linewidth vs. front facet reflectivity of 780 nm DFB diode lasers at high optical output power, Appl. Sci. 8 (7) (2018) 1104.

[13] T.P. Nguyen, M. Schiemangk, S. Spießberger, et al., Optimization of 780 nm DFB diode lasers for high-power narrow linewidth emission, Appl. Phys. B 108 (4) (2012) 767–771.

[14] M. Maiwald, Götz. Erbert, A. Klehr, et al., Monolithic DFB laser diodes emitting at 785 nm for in situ SER spectroscopy, Adv. Environ. Chem. Biol. Sensing Technol. III 5993 (2005) 599305-599305-10.

[15] M. Maiwald, G. Erbert, A. Klehr, et al., Reliable operation of 785 nm DFB diode lasers for rapid Raman spectroscopy, in: High-Power Diode Laser Technology and Applications V, Vol. 6456, International Society for Optics and Photonics, 2007, p. 64560W.

[16] A. Reinhold, M. Fischer, W. Zeller, et al., Evanescently coupled DBR laser arrays in the 760–770 nm wavelength range, IEEE Photonics Technol. Lett. 31 (16) (2019) 1319–1322.

[17] K. Nechay, H. Kahle, J.P. Penttinen, et al., AlGaAs/AlGaInP VECSELS with direct emission at 740–770 nm, IEEE Photonics Technol. Lett. 31 (15) (2019) 1245–1248.

[18] S. Nilsson, T. Kjellberg, T. Klinga, R. Schatz, J. Wallin, K. Streubel, Improved spectral characteristics of MQW-DFB lasers by incorporation of multiple phase-shifts, J. Lightwave Technol. 13 (1995) 434–441.

[19] H. Soda, H. Ishikawa, H. Imai, Design of DFB lasers for high-power single-mode operation, Electron. Lett. 22 (1986) 1047–1049.

[20] L.J.P. Ketelsen, I. Hoshino, D.A. Ackerman, Experimental and theoretical evaluation of the CW suppression of TE side modes in conventional 1.55$\mu m$ InP-InGaAsP distributed feedback lasers, IEEE J. Quantum Electron. 27 (1991).

[21] F. Gao, L. Qin, Y. Chen, et al., Study of gain-coupled distributed feedback laser based on high order surface gain-coupled gratings, Opt. Commun. 410 (2018) 936–940.

[22] Y. Chen, P. Jia, J. Zhang, et al., Gain-coupled distributed feedback laser based on periodic surface anode canals, Appl. Opt. 54 (30) (2015) 8863.

[23] K. David, G. Morthier, P. Vankwikelberge, et al., Gain-coupled DFB lasers versus index-coupled and phase shifted DFB lasers: a comparison based on spatial hole burning corrected yield, IEEE J. Quantum Electron. 27 (6) (1991) 0–1723.
[24] Sang-Taek Kim, Boo-Gyoun Kim, Analysis of single-mode yields above threshold for complex-coupled distributed feedback lasers with asymmetric facet reflectivities, J. Opt. Soc. Amer. B (2005).
[25] N. Susa, Fluctuations of the laser characteristics and the effect of the index-coupling component in the gain-coupled DFB laser, IEEE J. Quantum Electron. 33 (1997) 2255–2265.
[26] A.J. Lowery, D. Novak, Performance comparison of gain-coupled and index-coupled DFB semiconductor lasers, IEEE J. Quantum Electron. 30 (1994) 2051–2063, IEEE Photonics Technology Letters.
[27] https://www.toptica-eagleyard.com/products/single-frequency-laser-diodes/.
[28] https://nanoplus.com/en/products/distributed-feedback-lasers/760-nm-830-nm/.
[29] F. Gao, L. Qin, Y. Chen, et al., Two-segment gain-coupled distributed feedback laser, IEEE Photonics J. PP (99) (2018) 1–1.
[30] J. Decker, P. Crump, J. Fricke, et al., Narrow stripe broad area lasers with high order distributed feedback surface gratings, IEEE Photonics Technol. Lett. 26 (8) (2014) 829–832.
[31] H. Virtanen, T. Uusitalo, M. Karjalainen, et al., Narrow-linewidth 780-nm DFB lasers fabricated using nanoimprint lithography, IEEE Photonics Technol. Lett. PP (99) (2017) 1–1.